

NUMERICAL EVALUATION OF WEAKLY TURBULENT FLOW PATTERNS OF NATURAL CONVECTION IN A SQUARE ENCLOSURE WITH DIFFERENTIALLY HEATED SIDE WALLS

Jianlei Niu

*Department of Building Services Engineering,
The Hong Kong Polytechnic University, Kowloon,
Hong Kong, Peoples' Republic of China*

Zuojin Zhu

*Department of Thermal Science and Energy Engineering, School of Engineering
Science, University of Science and Technology of China, Hefei,
Peoples' Republic of China*

This article presents the results of numerical evaluation of weakly turbulent natural convection of air in a rectangular enclosure with differentially heated side walls and adiabatic horizontal walls. The turbulence in the natural convection was described by k - ϵ equations, which were solved by Strang splitting, while average thermal and fluid flow fields were described by statistically averaged equations, which were solved by the projection method PmIII. The combined application of projection method and the Strang splitting characterizes the numerical method in this study. Numerical results for Rayleigh number 1.58×10^9 have revealed reasonable agreement with the existing experimental ones, with some discrepancy attributable to the adiabatic boundary conditions on the horizontal walls. The results are also in good agreement with some published numerical results, particularly at higher Rayleigh numbers. However, comparison with the latest experimental data reveals that the turbulent heat flux model is not quite capable of giving satisfactory temperature distribution.

1. INTRODUCTION

Natural convection in rectangular enclosures has been extensively studied experimentally and numerically, owing to the wide engineering applications such as building ventilation and air conditioning, cooling of electronic devices and solar collectors, and nuclear reactor subsystems. There are many works simulating natural convection in enclosures, some of which have further included the interaction

Received 23 July 2003; accepted 22 September 2003.

This work was financially supported by Hong Kong RGC under Grant Polyu5031/01E.

Address correspondence to Jianlei Niu, Department of Building Services Engineering, The Hong Kong Polytechnic University, Kowloon, Hong Kong, Peoples' Republic of China. Email: Bejlniu@polyu.edu.hk.

NOMENCLATURE

$C_i, i = 1, 2, 3$	coefficients used in turbulence model	w	velocity component in z direction
C_p	specific heat under constant pressure	β_T	coefficient of volumetric expansion
Ec	Eckert number ($= w_0^2 / C_p \Delta T$)	$\delta\varepsilon$	dissipation rate increment during a half temporal step
\mathbf{g}	gravitational acceleration, m^2/s	$\Delta T = T_h - T_c$	temperature difference between the two vertical walls
G_k	turbulence production term due to turbulent heat flux	ε	dissipation rate of k
k	normalized turbulence kinetic energy	Θ	normalized temperature
H	width of the square enclosure m	ν_t	turbulent kinematic viscosity
$L (= H)$	height of the square enclosure m	ν	molecular kinematic viscosity, m^2/s
Nu_{av}	overall Nusselt number	ρ	mean density of the fluid, kg/m^3
P	pressure	$\sigma_\theta, \sigma_k, \sigma_\varepsilon$	turbulent Prandtl number of $\Theta, k,$ and ε
P_k	turbulence production term due to Reynolds stresses	τ_0	time scale of the dissipation of k
Pr	Prandtl number of fluid		
R	source term		
Ra	Rayleigh number	Superscripts	
S_1, S_2	solution operator in Strang splitting	n	temporal level
t_0	time scale, s	$*$	first half time level
t	time	$**$	result from solution operator S_2
T_c	absolute temperature of the cold vertical wall, K	Subscripts	
T_h	absolute temperature of the hot vertical wall, K	c	cold
\mathbf{u}	velocity vector	h	hot
v	velocity component in y direction	k	turbulent kinetic energy k
w_0	velocity scale, m/s	v	velocity component v
		w	velocity component w
		ε	dissipation rate of k
		Θ	temperature Θ

between radiation and natural convection, such as the recent work by Velusamy et al. [1]. Earlier numerical simulations of turbulent natural convection in a square enclosure with differential heated side walls and insulated horizontal walls were conducted by de Vahl Davis and Jones [2]. Since it is difficult to realize identical conditions in experiment to those in numerical simulation, there were discrepancies between the results of computation and measurement. Experimentalists have noticed the effect of the thermal boundary conditions on the horizontal walls upon the distribution of local Nusselt number on the vertical walls [3, 4]. A parametrical numerical study of this effect for the cases of Rayleigh number in the range 10^4 – 10^7 was reported by Ciofalo and Karayiannis [5]. It was indicated that the effect of thermal boundary condition on the horizontal walls is relevant, particularly for low-aspect-ratio enclosures.

Another earlier work was carried out by Ozoe et al. [6]. They studied numerically the laminar natural convection of water for Rayleigh numbers ranging from 10^6 to 10^9 , for Prandtl numbers 5.12 and 9.17, and turbulent natural convection of water for Rayleigh numbers in the range from 10^9 to 10^{11} and Prandtl number 6.7. The calculations for the laminar regime were consistent with the measurements

of Churchill [7]. They revealed the sensitivity of the parameters used in the adopted k - ϵ turbulence model.

In the past decade, Fusegi et al. [8] have studied three-dimensional natural convection in a side-wall-heated cube. The computational results were summarized in terms of correlations for overall Nusselt numbers with Rayleigh numbers. An excellent literature review of the numerical study of turbulent natural convection in enclosures was presented by Henkes and Hoogendoorn [9], in which a reference solution for the k - ϵ model by means of transition triggering was also obtained for the standard case of natural convection of air at a Rayleigh number of 5×10^{10} in a square enclosure, differentially heated with adiabatic horizontal walls.

Ince and Launder [10] investigated the three-dimensional and heat loss effect on turbulent flow in a nominally two-dimensional enclosure, using the k - ϵ model they reported earlier [11]. It was reported that accounting for heat loss from nominally adiabatic walls or for 3-D effects led to much closer agreement with experiment than hitherto. Le Quéré and co-workers [12, 13] applied the Chebyshev expansion method [14] in the study of 2-D and 3-D natural convection in enclosures, and explored the chaotic patterns as well as the three-dimensional transition in natural convection. It was found that, from the direct numerical simulation of the unsteady two-dimensional equations, the results for the chaotic natural convection in a differentially heated, air-filled cavity of aspect ratio 4 are satisfactory. The application of Chebyshev-Fourier expansions for the three-dimensional transition of natural convection indicated that the strong three-dimensional mixing leaves no, or only weak, three-dimensional structures in the time-average nonlinear solution. Three-dimensional effects increase the maximum of the time- and depth-averaged wall heat transfer by 15%.

More recently, Dol and Hanjalić [15] carried out a study of turbulent natural convection in a side-heated near-cubic enclosure at a high Rayleigh number ($Ra = 4.9 \times 10^{10}$). Their numerical method was characterized by the use of total variation diminishing (TVD) for the treatment of convection terms in the corresponding governing equations for the problem considered. Apart from the complexity of three-dimensional flows, they adopted both the low-Rayleigh-number differential second-moment stress/flux closure (SMC) and the related k - ϵ (KEM) model for the modeling of turbulence of natural convection in the cubic enclosure. This study revealed that the SMC is superior to the KEM in capturing the strongly curved flow patterns in the corner regions, and in reproducing the 3-D effects caused by heat losses through the imperfectly insulated horizontal walls. However, the SMC model is much more complicated than the more widely used KEM, and the solution requires much more computational resources.

On the other hand, Mergui and Penot [16] studied experimentally the natural convection of air in a differentially heated square cavity at Rayleigh number of 1.69×10^9 . They examined the temperature fields in the vicinity of the ceiling and the floor which allow the characterization of the actual boundary conditions on these walls. They also determined an analytic law for the temperature distribution along each horizontal wall, and presented flow visualizations by using laser tomography and spectral analysis of the time-dependent signal of the temperature recorded at several characteristic points in the cavity. It was found that there appears unsteadiness and a complex interaction between internal gravity waves, thermal

instabilities along the floor, and Tollmien-Schlichting waves in the hot vertical boundary layer. However, it seems that they reported lower local heat transfer rates.

Tian and Karayiannis [17, 18] recently conducted an experimental study for low-turbulence natural convection in an air-filled square cavity at a Rayleigh number of 1.58×10^9 . They presented not only the thermal and fluid flow fields but also the turbulence quantities. It was found that, at this Ra number, the fluid in the cavity core is stationary and stratified, and two additional much smaller vortices appear at the hot top and cold bottom corners. The flow in the cavity was found to be limited in a narrow strip along the walls where velocity and temperature change sharply. Clearly, these measurements are useful not only for the construction of more elaborate turbulence models but also for the validation and calibration of numerical simulators coded for natural convection. They give a brief literature review for both experiments and numerical calculations for natural convection in enclosures.

The purpose of this article is to apply the projection method [19] and Strang splitting [20] to simulate the turbulent flow patterns of natural convection of air in a 2-D square enclosure with differentially heated side-walls and adiabatic horizontal walls. The widely used k - ε turbulence model will be applied to evaluate the turbulent viscosity. It is expected that the change of turbulent flow patterns at moderate Ra can cause the oscillation of the overall Nusselt number, and that the results of calculation with the combined numerical method may achieve good consistency with the latest experimental results [17, 18] and the recent 3-D computational results [8]. This work will help to indicate the potential for the application of such a numerical method in the treatment of other engineering problems.

The remaining text of this article is presented in the following way: Section 2 gives the governing equations and the numerical methods, attaching the assessment of the method with respect to the published results. Section 3 contains the results and discussion, in which the flow patterns at different Ra values and the comparison with current measurements are shown, and the conclusions are given in Section 4.

2. GOVERNING EQUATIONS AND NUMERICAL METHOD

2.1. Governing Equations

Consider the turbulent natural convection in a rectangular enclosure in a Cartesian coordinate system, in which y is the horizontal coordinate and z is the vertical coordinate. The origin is allocated at the right bottom corner. It is assumed that the turbulent kinetic energy k and its dissipation rate ε in natural convection can be adopted to present the turbulent viscosity, in which the transient terms are retained. For the problem considered, a schematic is depicted in Figure 1, where the enclosure is filled with a fluid with kinematic viscosity ν and thermal diffusivity κ . The fluid is induced to flow clockwise by the heat transfer from the hot left wall at temperature T_h to the right wall at temperature T_c . The horizontal walls are adiabatic. It is also assumed that the Boussinesq approximation is valid and can be used to simplify the momentum equations. Because of kinetic energy dissipation, the temperature equation should be supplemented with an additional term called the Eckert number, Ec.

Following the approach of Wakitani [21], we select $w_0 = \sqrt{g\beta_T H \Delta T}$ as the velocity scale, taking H as the length scale; hence the time scale should be

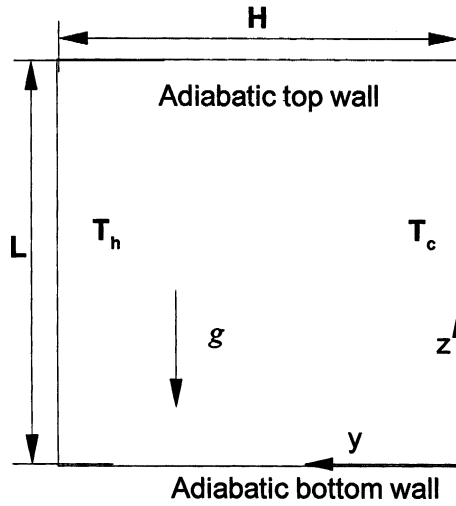


Figure 1. Schematic of the turbulent natural convection in a square enclosure differentially heated from side walls.

$t_0 = H/w_0 = \sqrt{\text{Pr}/\text{Ra}} H^2/\nu$, with ρw_0^2 being the measure of pressure. When we further define $\Theta = [T_h - (T_h + T_c)/2]/\Delta T$, introducing a general form for scalar variables $\phi (= \Theta, k, \text{ or } \varepsilon)$, the dimensionless governing equations for the turbulent natural-convection problem can be written as follows:

$$\phi_t + (\mathbf{u} \cdot \nabla)\phi = \nabla \cdot (\Gamma_\phi \nabla)\phi + R_\phi \tag{1}$$

with the continuity equation

$$\nabla \cdot \mathbf{u} = 0 \tag{2}$$

and vector-form momentum equation

$$\mathbf{u}_t + (\mathbf{u} \cdot \nabla)\mathbf{u} = -\nabla p + \Theta \lambda + \nabla \cdot (\Gamma_u \cdot \nabla)\mathbf{u} \tag{3}$$

where $\lambda = (0, 1)$ denotes the unit vector in the vertical direction, and Pr is the Prandtl number, with Rayleigh number $\text{Ra} = g\beta_T(T_h - T_c)H^3/(\nu\kappa)$. The diffusion coefficient Γ and the source term R_ϕ are shown in Table 1. It is noted that, in this study,

Table 1. Diffusion coefficients and source terms for governing equations

ϕ	Γ_ϕ	R_ϕ
Θ	$\frac{1}{\sqrt{\text{Pr Ra}}} + \frac{\nu_t}{\sigma_\Theta}$	$\text{Ec} \left(\sqrt{\frac{\text{Pr}}{\text{Ra}}} / \nu_t + 1 \right) P_k$
k	$\sqrt{\frac{\text{Pr}}{\text{Ra}}} + \frac{\nu_t}{\sigma_k}$	$P_k + G_k - \varepsilon$
ε	$\sqrt{\frac{\text{Pr}}{\text{Ra}}} + \frac{\nu_t}{\sigma_\varepsilon}$	$\frac{[C_1(P_k + C_3 G_k) - C_2 \varepsilon] \varepsilon}{k}$

the coefficients C_i , $i = 1, 2, 3$ were set as 1.44, 1.92, and 0.5; and the turbulent Prandtl numbers σ_Θ , σ_k , σ_ε were set as 0.9, 1.0, and 1.3, respectively.

The production terms for k contain two terms:

$$P_k = \nu_t \left[2 \left(\frac{\partial v}{\partial y} \right)^2 + 2 \left(\frac{\partial w}{\partial z} \right)^2 + \left(\frac{\partial v}{\partial z} + \frac{\partial w}{\partial y} \right)^2 \right]$$

and

$$G_k = - \frac{\nu_t}{\sigma_\Theta} \frac{\partial \Theta}{\partial z}$$

with turbulent kinematic viscosity

$$\nu_t = C_\mu \frac{k^2}{\varepsilon}$$

where C_μ equals 0.09.

The solutions of the governing equations (1–3) should be sought under appropriate conditions that are compatible with the problem considered. As mentioned earlier, the boundary conditions on the two vertical walls can be written as

$$v = 0 \quad w = 0 \quad \Theta = 0.5 \quad k = 0 \quad \varepsilon = 0 \quad \text{for } y = 1, z \in (0, 1) \quad (4)$$

and

$$v = 0 \quad w = 0 \quad \Theta = -0.5 \quad k = 0 \quad \varepsilon = 0 \quad \text{for } y = 0, z \in (0, 1) \quad (5)$$

For the horizontal walls, we have

$$v = 0 \quad w = 0 \quad \frac{\partial \Theta}{\partial z} = 0 \quad k = 0 \quad \varepsilon = 0 \quad \text{for } z = 0 \text{ or } 1, y \in (0, 1) \quad (6)$$

It should be noted that the boundary condition for the dissipation rate is in accordance with that initially proposed by Ince and Launder [10].

On the other hand, the initial conditions are simply assigned as

$$v = 0 \quad w = 0 \quad \Theta = 0 \quad k = 0 \quad \varepsilon = 10^{-5} \\ \text{for } t = 0, \text{ and } y \in (0, 1), z \in (0, 1) \quad (7)$$

The small initial value for turbulent kinetic dissipation rate is given for the convenience of turbulent viscosity evaluation. It should be noted that the source term in the Θ equation containing the $Ec (= w_0^2 / Cp \Delta T)$ number is very small in the problem considered. Thus, it may be ignored without causing any effect on the numerical solutions.

2.2. Solution Method

The solution method is characterized by the use of the projection method (PmIII) and Strang splitting (SS) schemes. The PmIII scheme, developed by Brown et al. [19], has been applied to evaluate the multicellular patterns of laminar natural convection of air in a tall cavity [22] as well as to study the laminar natural convection in a parallel-walled channel [23]. It is adopted to obtain the temperature and velocity fields for the turbulent natural-convection problem at hand. Strang splitting was first reported by Strang [20], but was used recently in construction of high-order numerical methods for the space nonhomogeneous Boltzmann equation [24]. The Strang splitting method is applied here to provide the solutions of the k and ε equations.

Following the description of SS given by Filbet [24], it is well known that, in a small time interval $\Delta t = [t^n, t^{n+1}]$, for ϕ , the first-order splitting method gives

$$\frac{\partial \phi}{\partial t} = R_\phi(\phi^*) \tag{8}$$

with $\phi^*(0, y, z) = \phi^n(y, z)$, and

$$\frac{\partial \phi^{**}}{\partial t} = -[(\mathbf{u} \cdot \nabla)\phi]^{n+1/2} + \nabla \cdot (\Gamma_\phi \nabla \phi^{**}) \tag{9}$$

with $\phi^{**}(0, y, z) = \phi^*(\Delta t, y, z)$. If the numerical solution of the source term associated part is represented by

$$\phi^*(\Delta t, y, z) = S_1(\Delta t)\phi^n \tag{10}$$

and the solution of the convection-diffusion equation (9) is written as

$$\phi^{**}(\Delta t, y, z) = S_2(\Delta t)\phi^*(\Delta t, y, z) \tag{11}$$

The Strang splitting suggests that the solution with second-order accuracy can be expressed as

$$\phi^{n+1}(\Delta t, y, z) = S_1\left(\frac{\Delta t}{2}\right)S_2(\Delta t)S_1\left(\frac{\Delta t}{2}\right)\phi^n(y, z) \tag{12}$$

Considering the strong nonlinear property and the interaction between k and ε , with the Strang splitting, the details of the solution for k and ε can be given below. The operator $S_1(\Delta t/2)$ acting on $(k, \varepsilon)^n$ gives

$$\begin{cases} \varepsilon^* = \varepsilon^n + \delta\varepsilon \\ k^* = k^n + (R_k - \delta\varepsilon)\Delta t/2 \end{cases} \tag{13}$$

where $\delta\varepsilon = R_\varepsilon\tau_0/(2\tau_0/\Delta t + C_2)$ and $\tau_0 = k^n/\varepsilon^n$.

Applying $S_2(\Delta t)$ on $(k, \varepsilon)^*$ yields the solutions of the source-term-removed equations:

$$\frac{\partial k}{\partial t} + \frac{\partial vk}{\partial y} + \frac{\partial wk}{\partial z} = \frac{\partial}{\partial y} \left(\Gamma_k \frac{\partial k}{\partial y} \right) + \frac{\partial}{\partial z} \left(\Gamma_k \frac{\partial k}{\partial z} \right) \quad (14)$$

$$\frac{\partial \varepsilon}{\partial t} + \frac{\partial v\varepsilon}{\partial y} + \frac{\partial w\varepsilon}{\partial z} = \frac{\partial}{\partial y} \left(\Gamma_\varepsilon \frac{\partial \varepsilon}{\partial y} \right) + \frac{\partial}{\partial z} \left(\Gamma_\varepsilon \frac{\partial \varepsilon}{\partial z} \right) \quad (15)$$

The solutions are denoted by $(k, \varepsilon)^{**}$. The final step, giving the solutions $(k, \varepsilon)^{n+1}$, is as follows:

$$\begin{cases} \varepsilon^{n+1} = \varepsilon^{**} + \delta\varepsilon^{**} \\ k^{n+1} = k^{**} + (R_k^{**} - \delta\varepsilon^{**})\Delta t/2 \end{cases} \quad (16)$$

where $\delta\varepsilon^{**} = R_\varepsilon^{**}\tau_0^{**}/(2\tau_0^{**}/\Delta t + C_2)$ and $\tau_0^{**} = k^{**}/\varepsilon^{**}$. It should be noted that the convective terms in the governing equations are spatially differenced by a second-order upwind scheme on a nonuniform staggered grid whose minimum mesh size near the walls is about 9.0×10^{-4} ; these terms are obtained explicitly by using the second-order Adams-Bashforth formula. The source terms in the k and ε equations are treated semi-implicitly.

2.3. Method Assessment and Grid Independence Inspection

The numerical method presented above was assessed by considering the natural turbulent convection of air for $\text{Ra} = 1.58 \times 10^9$ in a square enclosure with differentially heated side walls, while its upper and lower walls are adiabatic (schematic shown in Figure 1). A similar situation has been experimentally studied recently by Tian and Karayiannis [17, 18]. The initial value of temperature Θ in the enclosure was zero.

The results of the grid-independence inspection are given in Table 2. It is seen that, for the finest grid, a small change of temporal step does not affect the overall Nusselt number ($\text{Nu}_{\text{av}} = (1/H) \int_0^H (\partial\Theta/\partial y)|_{y=1} dz$). Figure 2 shows the convergence history with the evolution of overall Nusselt number evaluated for the four different nonuniform staggered grids given in Table 2, when the temporal step was set as 4×10^{-3} . It is seen that, even at the temporal instant $t = 400$, the absolute difference

Table 2. Grid dependence of numerical results for $\text{Ra} = 1.58 \times 10^9$

Grid	Δt	$\text{Nu}_{\text{av}} (t = 280)$
31×31	4×10^{-4}	65.228
41×41	4×10^{-4}	66.472
61×61	4×10^{-4}	68.030
81×81	4×10^{-4}	68.576
81×81	3×10^{-4}	68.572
81×81	5×10^{-4}	68.582

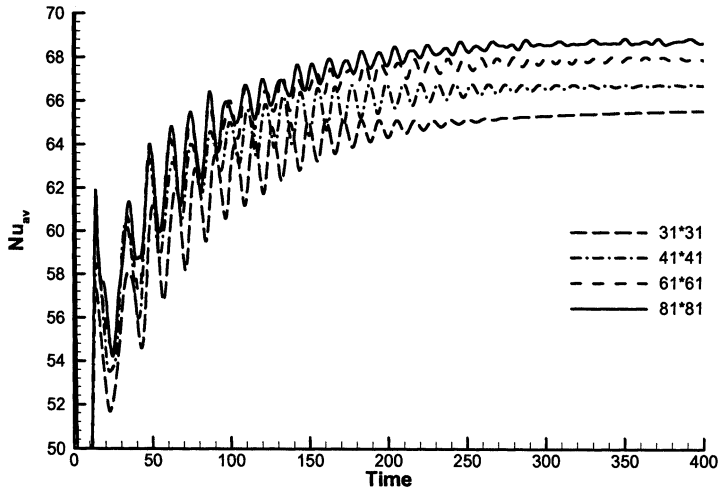


Figure 2. Convergence history with the evolution of overall Nusselt number for $Ra = 1.58 \times 10^9$ under different grid systems.

between the Nusselt number for grid sizes 61×61 and 81×81 is about unity, implying that the relative deviation is less than 2%. The Nusselt number is almost independent of the numerical grid when the grid size is as large as 81×81 . The convergence history indicates that the overall Nusselt number has a temporal oscillation resulting from the change of transitional flow patterns of natural convection in the square enclosure.

For the measured value of the overall Nusselt number, Tian and Karayiannis [17] obtained 64.0 for the hot wall and 65.3 for the cold wall. However, Mergui and Penot [16] obtained lower overall Nusselt number than the values measured by Tian et al. Our calculation has shown that at $Ra = 1.58 \times 10^9$ in terms of the adiabatic horizontal walls, the overall Nusselt number is 68.6, illustrating a discrepancy with recent measurement of about 7%. For the case with heat loss from the horizontal walls whose surface temperature on the wall surfaces is given in Table 3, at $Ra = 1.58 \times 10^9$, the average Nusselt number is 61.67 for the hot wall and 60.29 for

Table 3. Surface temperature on the bottom and top horizontal walls for the case with heat loss at $Ra = 1.58 \times 10^9$ with respect to [17]

y	$\Theta (z = 0)$	$\Theta (z = 1)$	y	$\Theta (z = 0)$	$\Theta (z = 1)$
1	0.5	0.5	0.306818	-0.19318	0.107955
0.897727	0.397727	0.431818	0.267045	-0.23295	0.056818
0.892045	0.392045	0.420455	0.238636	-0.26136	-0.00568
0.857955	0.357955	0.414773	0.145455	-0.35455	-0.17045
0.767045	0.267045	0.397727	0.090909	-0.40909	-0.28409
0.656818	0.156818	0.318182	0.039773	-0.46023	-0.36364
0.520455	0.020455	0.255682	0.034091	-0.46591	-0.36932
0.443182	-0.05682	0.204545	0.022727	-0.47727	-0.39773
0.386364	-0.11364	0.170455	0	-0.5	-0.5
0.340909	-0.15909	0.130682			

the cold wall. Thus, it is evident that the calculated average Nusselt number for the hot and cold walls is sensitive to the thermal boundary conditions on the top and bottom horizontal walls. The present results are in good agreement with the measured data. As indicated in [5] for lower-Ra cases, the heat loss from horizontal walls is the important reason that may cause lower Nusselt number from numerical calculation.

3. RESULTS AND DISCUSSION

The numerical results were obtained by means of the nonuniform 81×81 grid and the 4×10^{-3} temporal step. The finest mesh size close to the walls was about 9×10^{-4} . For higher Rayleigh numbers, the computation was terminated at the instant $t = 400$, while for other cases, the termination was done at $t = 200$. This study reveals the features listed below.

1. Even for turbulent natural convection, there do exist transient flow patterns involved with the vortex motion.
2. The $k-\epsilon$ model, if used with appropriate boundary conditions, can show fairly satisfactory numerical solutions for the problem considered.
3. The use of Strang splitting can give rise to reasonable results.

3.1. Comparison with Measurement

The comparison of the present numerical results with measurement was mainly carried out for the case of $Ra = 1.58 \times 10^9$. Apart from the overall Nusselt number discussed in Subsection 2.3, what is presented here will include the velocity and temperature profiles, the wall shear stresses, and the local Nusselt number ($Nu_z = \partial\Theta/\partial y|_{y=1}$) for a given location z on the hot wall.

Shown in Figure 3 is the velocity profile near the vertical walls at the middle-height section $z = 0.5$, in which both the measurement results by Tian and

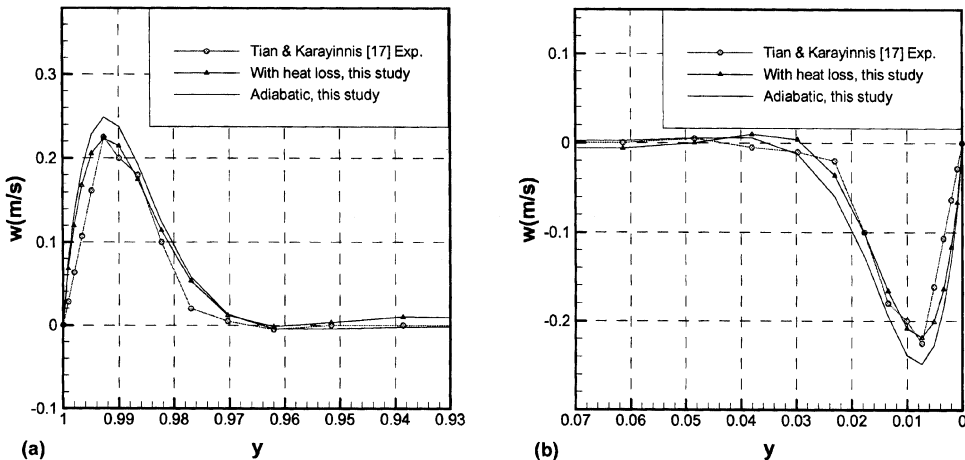


Figure 3. Comparison of velocity component w at $z = 0.5$ for $Ra = 1.58 \times 10^9$.

Karayiannis [17] and the numerical results obtained in this study are included. It can be seen that for the case of adiabatic horizontal walls the maximum deviation appears at the peaks, which is about 0.02 m/s. If heat loss from the horizontal walls is permitted, by using the surface temperature shown in Table 3, the calculated peak value of the velocity profile is almost identical to the measured value. The overall comparison shows that the calculated velocity profile w ($z=0.5$) is in good agreement with the measured one.

Figure 4 gives the comparison of temperature profile near the two vertical walls. The discrepancy between the calculated and measured temperature profiles may be attributed to the physical model for the turbulent heat flux. Nevertheless, the comparison also indicates overall good agreement between the results of calculation and measurement.

The satisfactory performance of the present numerical method can also be observed from the comparison of the wall shear stresses and the local Nusselt number on the hot wall, as shown in Figures 5 and 6. From Figure 5, it is seen that, for the case of adiabatic horizontal walls, the calculated wall shear stresses on the hot and cold walls are symmetric with respect to the point $z=0.5$. However, the permission of heat loss from the horizontal walls can make a wavy distribution in the bottom region for the hot wall and in the top region for the cold wall, implying that the heat loss has certainly changed the flow patterns at the particular Rayleigh number $Ra = 1.58 \times 10^9$. In comparison, the measured shear stresses are distorted to be asymmetrical, most likely due to the presence of asymmetrical heat loss from the horizontal walls. However, good agreement for the shear stresses is observable.

Figure 6 presents the local Nusselt number along the vertical hot wall, from which it can be seen that the curve given by Mergui and Penot [16] indicates that the heat transfer rate measured is lower. In the central region of the vertical wall, the calculated values of local Nusselt number show very good agreement with the measured values of Tian and Karayiannis [17]. The evident deviations near the top and bottom regions can certainly be explained as the result of the influence of heat losses from the horizontal walls on the measurements.

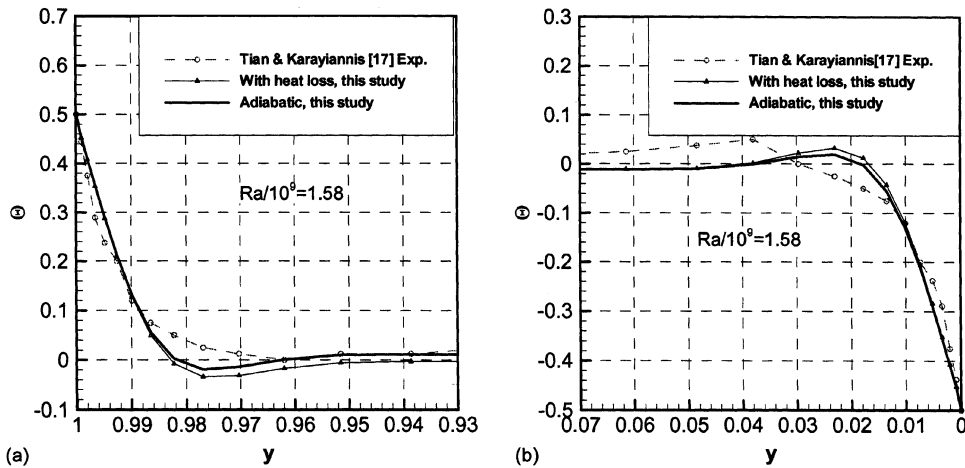


Figure 4. Comparison of temperature at $z = 0.5$ for $Ra = 1.58 \times 10^9$.

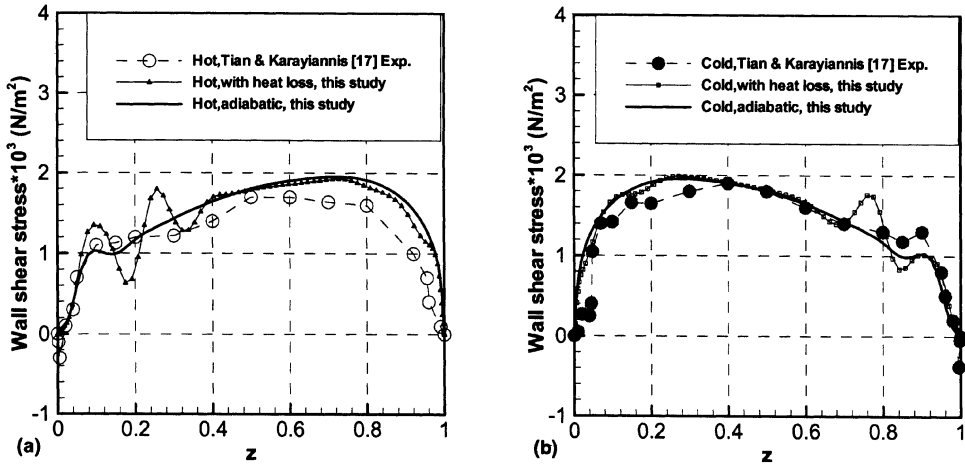


Figure 5. Comparison of shear stresses on the hot and cold walls for $Ra = 1.58 \times 10^9$.

3.2. Turbulent Flow Patterns

The flow patterns discussed in this subsection are obtained by using the adiabatic condition on the horizontal walls. In Figure 2 the convergence history is illustrated, and it is seen that the calculated overall Nusselt number shows evident oscillation over the evolution time. What is the reason for the variation of heat transfer rate across the hot wall? The change of turbulent flow patterns, i.e., flow pattern evolution, may be the driving source, since this change may lead to variation of the temperature gradient near the vertical hot wall.

To show the flow patterns, it is convenient to define a stream function ψ , which can give rise to the velocity components by its partial derivatives, i.e.,

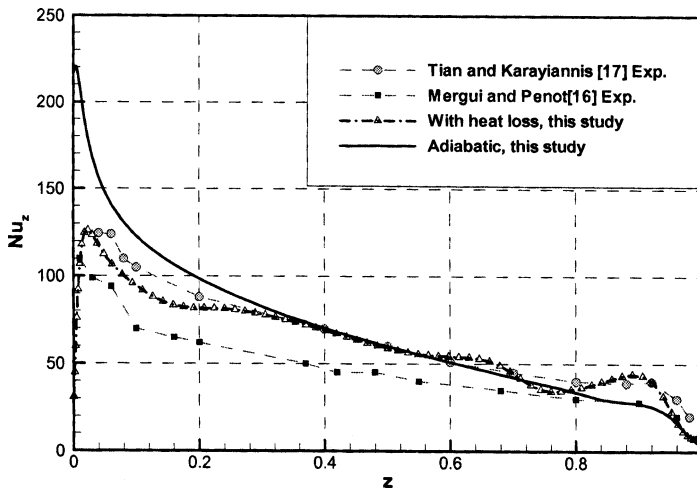


Figure 6. Comparison of local Nusselt number on the hot wall for $Ra = 1.58 \times 10^9$.

$$v = \frac{1}{\sqrt{Ra Pr}} \frac{\partial \psi}{\partial z} \quad w = -\frac{1}{\sqrt{Ra Pr}} \frac{\partial \psi}{\partial y}$$

For the benchmark problem of natural convection in the laminar case at $Ra = 10^7$, the iso-streamlines labeled by such ψ -function values were obtained and reported by Le Quéré et al. [14] using the Chebyshev method. In this study, we define the stream function in the same way as Le Quéré, for the convenience of comparison.

Generally, we select the case of $Ra = 10^9$ as an example to see how the turbulent flow patterns change during a given temporal range from 100 to 130. Figure 7 illustrates the flow patterns at four instants: $t = 100, 110, 120$, and 130 . It is noted that the flow patterns in the core region show significant variation as time increases. The patterns at the four instants are symmetric to the central point $(0.5, 0.5)$. In the

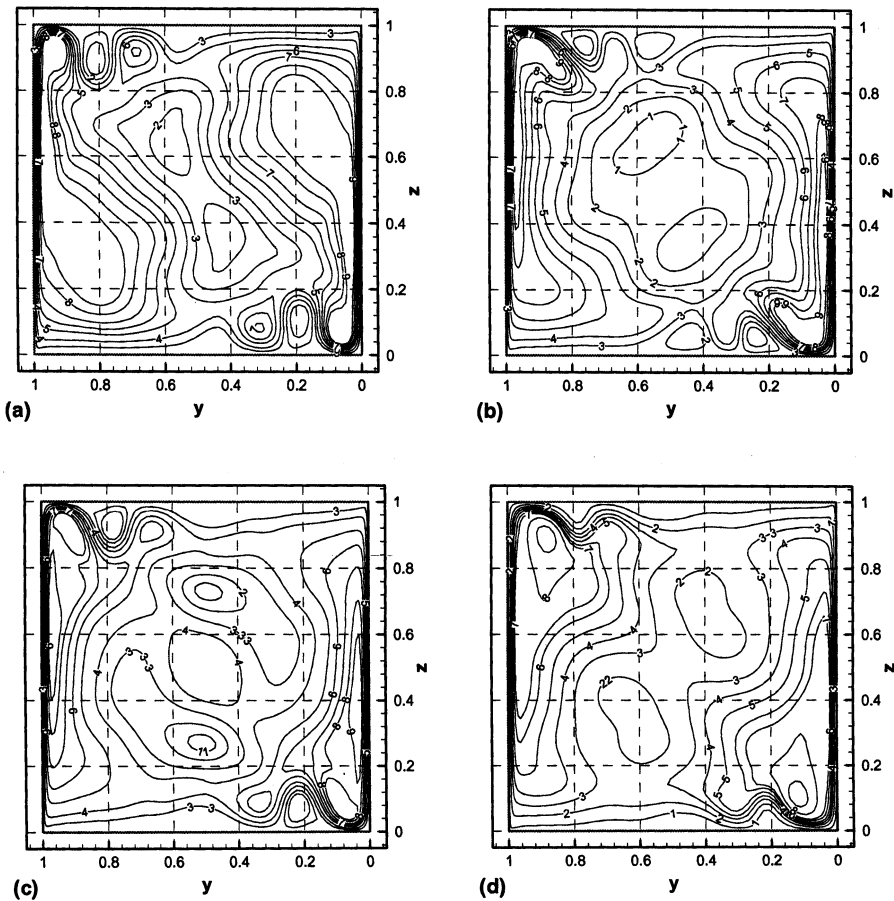


Figure 7. Iso-streamlines for $Ra = 10^9$ at the instants: (a) $t = 100$, with the labeled curves corresponding to streamfunction values $-20, -5, 10, 25, 45, 60, 75, 90$, and 100 ; (b) $t = 110$, with the labeled curves related to the same values of streamfunction as given in (a); (c) $t = 120$, where the first labeled curve has the Ψ value -15 , and the other labeled curves have the same Ψ values as in (a); (d) $t = 130$, where the labeled curves are related to Ψ values $5, 25, 45, 60, 75, 90, 125$, and 160 .

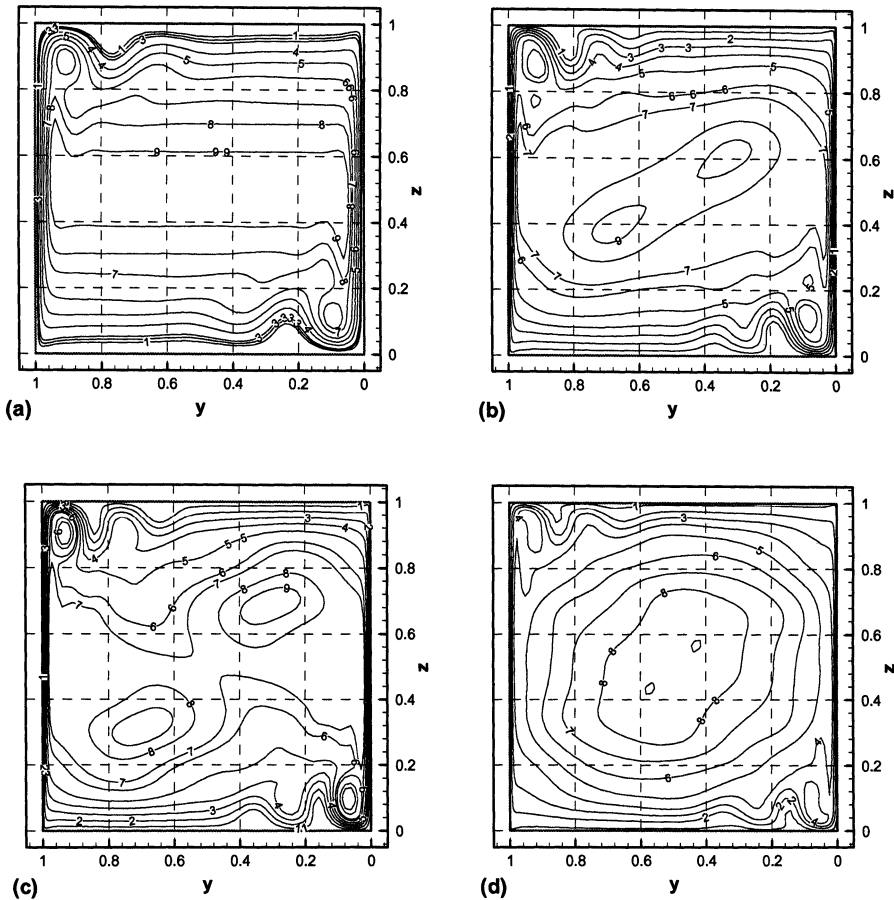


Figure 8. Iso-streamlines at the instant $t=200$ for (a) $Ra=10^8$ with the labeled curves corresponding to streamfunction values 5, 7.5, 10, 20, 30, 40, 50, 55, 60; (b) $Ra=10^9$, with the labeled curves relevant to streamfunction values 5, 20, 40, 60, 80, 100, 110, 130, 140; (c) $Ra=1.58 \times 10^9$, with the labeled curves relevant to the same values as in (b); (d) $Ra=5.58 \times 10^9$, with the labeled curves relevant to the streamfunction values 5, 50, 100, 150, 200, 250, 300, 350, 405.

patterns corresponding to the instants $t=100$, 110, and 120, there exist flow separation and reattachment in the boundary layers on the horizontal walls. This appears near the left top and right bottom corner regions, where vortexes labeled with negative ψ values can be observed. However, at $t=130$, the corner vortexes merely induce the evident streamline distortion; they do not cause flow separation and reattachment in the top and bottom boundary layers.

For the cases at different Rayleigh numbers, at the instant $t=200$, the turbulent flow patterns of natural convection of air in a differentially heated square enclosure are presented in Figure 8. It is evident that the heat transfer rate across the hot wall has important influence on the turbulent flow patterns of natural convection.

However, in contrast to the obvious differences in the flow patterns, the iso-therms depicted in Figure 9 have more simple structures. By close observation, it is

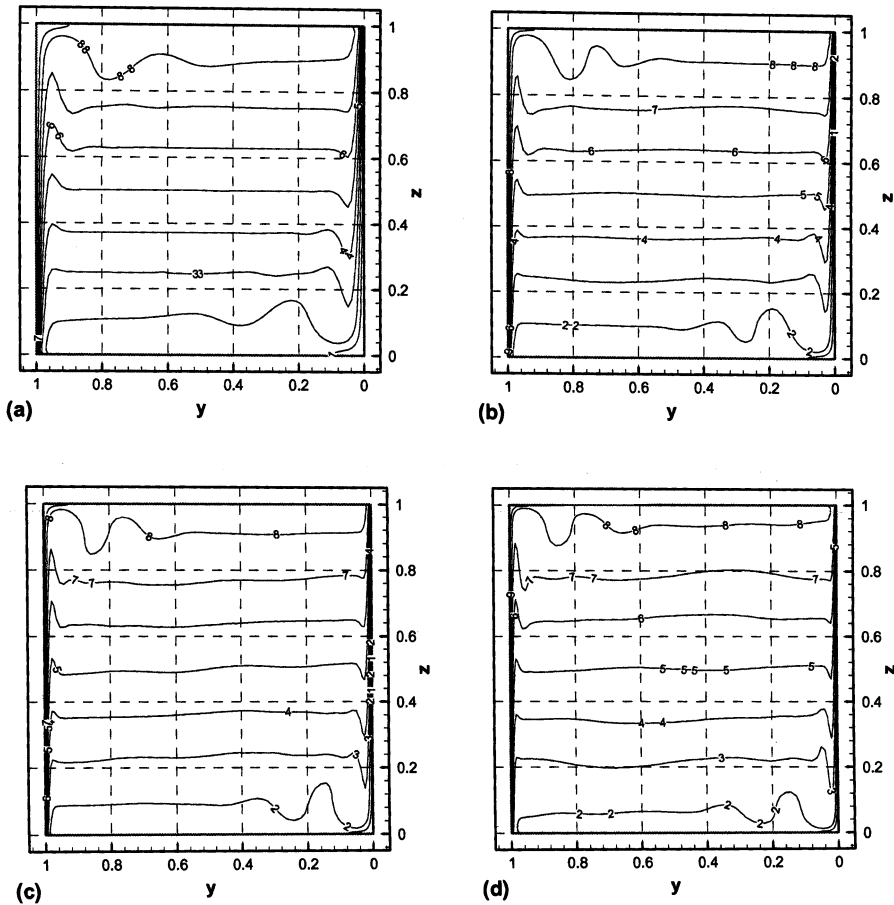


Figure 9. Iso-therms at the instant $t=200$ for (a) $Ra=10^8$; (b) $Ra=10^9$; (c) $Ra=1.58 \times 10^9$; (d) $Ra=5.58 \times 10^9$. Note that the labeled curves correspond to the Θ value -0.4 via 0 to 0.4 with an increment 0.1 .

noted that the distortion and varying trend are certainly closely related to the turbulent flow patterns shown in Figure 8.

3.3. Overall Nusselt Number

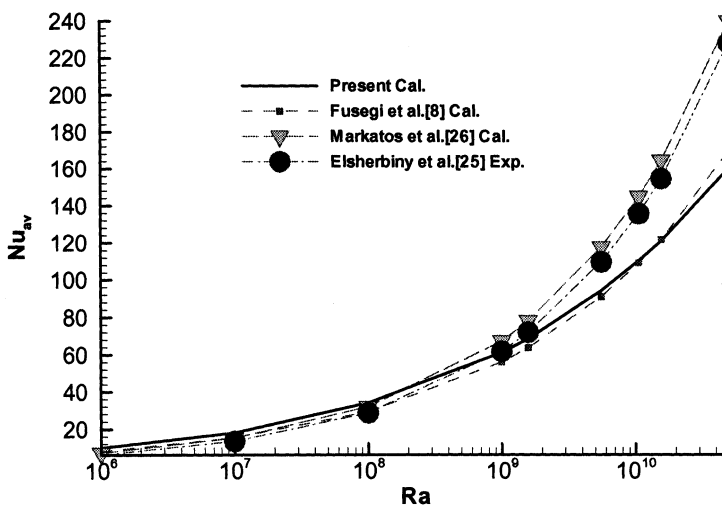
Table 4 shows the overall Nusselt numbers at different Rayleigh numbers. The values calculated by the correlation of Elsherbiny et al. [25] are given in the third column, while the overall Nusselt numbers calculated with present numerical method for the cases with adiabatic horizontal walls are shown in the second column. The results obtained numerically and reported by Markatos et al. [26] and Fusegi et al. [8] are given in the fourth and fifth columns, respectively. It can be seen that the present calculation results are in good agreement with the results reported by Fusegi et al. The results given in Table 4 are also shown in Figure 10.

Table 4. Overall Nusselt number Nu_{av} at different Ra

Ra	Present calculation	Elsherbiny et al. [25] $0.062 \times Ra^{1/3}$ (experimental)	Markatos et al. [26] $0.082 \times Ra^{0.324}$ (numerical)	Fusegi et al. [8] $0.163 \times Ra^{0.282}$ (numerical)
10^6	9.81	6.20	7.21	8.02
10^7	18.03	13.4	15.20	15.35
10^8	34.06	28.8	32.05	29.39
10^9	61.00	62.0	67.58	56.26
1.58×10^9	68.58	72.2	78.38	64.00
5.58×10^9	94.56	110.0	117.96	91.36
1.058×10^{10}	110.62	136.0	145.13	109.42
1.558×10^{10}	121.32	154.8	164.52	122.04
5×10^{10}	160.47	228.4	240.04	169.55

For the case $Ra = 10^7$, for laminar natural convection in a differentially heated square enclosure, using the Chebyshev method, Le Quéré reported an overall Nusselt number of 16.52. In the present simulation, the simulated Nusselt number is 18.02, which is an overestimation of about 9%.

Markatos et al. [26] obtained results for the natural-convection problem using wall functions, but Tian and Karayiannis [17] noted that such an application may cause a nonunique numerical solution. With regard to the overall Nusselt numbers, the difference between the present method and that of Markatos appears to be large at higher Rayleigh number. On the other hand, the present simulation presents really a excellent agreement with the results of Fusegi et al. [8], which were obtained for the natural convection of air in a differentially heated cube. In the Ra range from 10^6 to 10^{10} , the results from all three different numerical studies are quite comparable with the measured results. For the case of Ra beyond 10^9 , the larger deviation that can be seen in Figure 10 may be related to the numerical viscosity, which can exhibit its

**Figure 10.** Comparison of the overall Nusselt number with the reported results.

influence more conveniently for the large-Ra cases. The influence of numerical viscosity should be the inevitable feature that may cause lower-biased temperature gradient near the walls. A reasonable way to tackle such a discrepancy for the case of higher Ra is to employ a wall function. It is with this consideration that the comparison of different turbulence models by Henkes and Hoogendoorn [27] exhibits the most relevant significance.

4. CONCLUSIONS

This article has presented a numerical evaluation of weakly turbulent flow patterns of natural convection of air in a differentially heated square enclosure with a PmIII-SS joint method. By means of the projection method PmIII, the numerical solutions for the temperature and velocity fields were obtained; by means of the Strang splitting, the numerical solutions for the turbulent kinetic energy and the energy dissipation rate were found. Detailed comparison with more recent experimental results was carried out, including the velocity and temperature profiles, the wall shear stresses, and the local Nusselt number for the natural convection of air in a cube with differentially heat vertical walls at a Rayleigh number of 1.58×10^9 . Considering that there exist differences in the boundary conditions on the horizontal walls, the application of the joint method has proved to be able to obtain numerical results that are in good agreement with the measured data. The comparison with the latest experimental data reveals that the turbulent heat flux model used is not quite capable of giving satisfactory temperature distribution. It is estimated that the numerical method can be used widely in engineering problems, such as the simulation of air flow within building spaces and around buildings.

REFERENCES

1. K. Velusamy, T. Sundararajan, and K. N. Seetharamu, Interaction Effects between Surface Radiation and Turbulent Natural Convection in Square and Rectangular Enclosures, *ASME J. Heat Transfer*, vol. 123, pp. 1062–1070, 2001.
2. G. De Vahl Davis and I. P. Jones, Natural Convection in a Square Cavity: A Comparison Exercise, *Int. J. Numer. Meth. Fluids*, vol. 3, pp. 227–248, 1983.
3. S. M. Elshebiny, K. G. T. Hollands, and G. D. Raithby, Effect of Thermal Boundary Conditions on Natural Convection in Vertical and Inclined Air Layer, *ASME J. Heat Transfer*, vol. 104, pp. 515–520, 1982.
4. S. M. Bajorek and J. R. Floyd, Experimental Investigation of Natural Convection in Partitioned Enclosures, *ASME J. Heat Transfer*, vol. 104, pp. 527–531, 1982.
5. M. Ciofalo and T. G. Karayiannis, Numerical Convection Heat Transfer in a Partially or Completely Partitioned Vertical Rectangular Enclosure, *Int. J. Heat Mass Transfer*, vol. 34, no.1, pp. 167–179, 1991.
6. H. Ozoe, A. Mouri, M. Ohmuro, S. W. Chuechill, and N. Lior, Numerical Calculation of Laminar and Turbulent Natural Convection in Water in Rectangular Channels Heated and Cooled Isothermally on the Opposing Vertical Walls, *Int. J. Heat Mass Transfer*, vol. 28, pp. 125–138, 1985.
7. S. W. Churchill and R. Usagi, A General Expression for the Correlation of Rates of Transfer and Other Phenomena, *AIChE J.*, vol.18, pp. 1121–1128, 1972.
8. T. Fusegi, J. M. Hyun, and K. Kuwahara, Transient Three-Dimensional Natural Convection in a Differentially Heated Cubical Enclosure, *Int. J. Heat Mass Transfer*, vol. 34, pp. 1559–1564, 1991.

9. R. A. W. M. Henkes and C. J. Hoogendoorn, Comparison Exercise for Computations of Turbulent Natural Convection in Enclosures, *Numer. Heat Transfer B*, vol. 28, pp. 59–78, 1995.
10. N. Z. Ince and B. E. Launder, Three-Dimensional and Heat-Loss Effects on Turbulent Flow in a Nominally Two-Dimensional Cavity, *Int. J. Heat Fluid Flow*, vol. 16, pp. 171–177, 1995.
11. N. Z. Ince and B. E. Launder, On the Computation of Buoyancy-Driven Turbulent Flows in Rectangular Enclosures, *Int. J. Heat Fluid Flow*, vol. 10, pp. 110–117, 1989.
12. S. Xin, and P. Le Quéré, Direct Numerical Simulations of Two-Dimensional Chaotic Natural Convection in a Differentially Heated Cavity of Aspect Ratio 4, *J. Fluid Mech.*, vol. 304, pp. 87–118, 1995.
13. R. A. W. M. Henkes and P. Le Quéré, Three-Dimensional Transition of Natural-Convection Flows, *J. Fluid Mech.*, vol. 319, pp. 281–303, 1996.
14. P. Le Quéré and A. De Roquefort, Computation of Natural Convection in Two-Dimensional Cavities with Chebyshev Polynomials, *J. Comput. Phys.*, vol. 57, pp. 210–228, 1985.
15. H. S. Dol and K. Hanjalic, Computational Study of Turbulent Natural Convection in a Side-Heated Near-Cubic Enclosure at a High Rayleigh Number, *Int. J. Heat Mass Transfer*, vol. 44, pp. 2322–2344, 2001.
16. S. Mergui and F. Penot, Natural Convection in a Differentially Heated Square Cavity: Experimental Investigation at $Ra = 1.69 \times 10^9$, *Int. J. Heat Mass Transfer*, vol. 39, pp. 563–574, 1996.
17. Y. S. Tian and T. G. Karayiannis, Low Turbulence Natural Convection in an Air Filled Square Cavity. Part I: The Thermal and Fluid Flow Fields, *Int. J. Heat Mass Transfer*, vol. 43, pp. 849–866, 2000.
18. Y. S. Tian and T. G. Karayiannis, Low Turbulence Natural Convection in an Air Filled Square Cavity. Part II: The Turbulence Quantities, *Int. J. Heat Mass Transfer*, vol. 43, pp. 867–884, 2000.
19. D. L. Brown, R. Cortez, and M. L. Minion, Accurate Projection Methods for the Incompressible Navier-Stokes Equations, *J. Comput. Phys.*, vol. 168, pp. 464–499, 2001.
20. G. Strang, On the Construction and Comparison of Difference Schemes, *SIAM J. Numer. Anal.*, vol. 5, pp. 506–517, 1968.
21. S. Wakitani, Development of Multicellular Solution in Natural Convection in a Air-Filled Vertical Cavity, *ASME J. Heat Transfer*, vol. 119, pp. 97–101, 1996.
22. Z. J. Zhu and H. X. Yang, Numerical Investigation of Transient Laminar Natural Convection of Air in a Tall Cavity, *Heat Mass Transfer*, vol. 39, pp. 579–587, 2003.
23. H. X. Yang and Z. J. Zhu, Numerical Study of Transient Laminar Natural Convection in an Inclined Parallel-Walled Channel, *Int. Commun. Heat Mass Transfer*, vol. 30, pp. 359–367, 2003.
24. F. Filbet and G. Russo, High Order Numerical Methods for the Space Non-homogeneous Boltzmann Equation, *J. Comput. Phys.*, vol. 186, pp. 457–480, 2003.
25. S. M. Elsherbiny, G. D. Raithby, and K. G. T. Hollands, Heat Transfer by Natural Convection across Vertical and Inclined Air Layers, *ASME J. Heat Transfer*, vol. 104, pp. 96–102, 1982.
26. N. C. Markatos and K. A. Pericleous, Laminar and Turbulent Natural Convection in an Enclosed Cavity, *Int. J. Heat Mass Transfer*, vol. 27, pp. 755–772, 1984.
27. R. A. W. M. Henkes and C. J. Hoogendoorn, Comparison of Turbulence Models for the Natural Convection Boundary Layer along a Heated Vertical Plate, *Int. J. Heat Mass Transfer*, vol. 32, no.1, pp. 157–169, 1989.

Copyright of Numerical Heat Transfer: Part A -- Applications is the property of Taylor & Francis Ltd and its content may not be copied or emailed to multiple sites or posted to a listserv without the copyright holder's express written permission. However, users may print, download, or email articles for individual use.